

Interaction between the Nazca and South American plates and formation of the Altiplano–Puna plateau: Review of a flexural analysis along the Andean margin (15°–34°S)

Andrés Tassara*

Institut für Geologische Wissenschaften, Freie Universität Berlin, Malteserstrasse 74-100, D-12249 Berlin, Germany

Received 15 November 2002; received in revised form 8 July 2003; accepted 23 December 2004

Available online 19 February 2005

Abstract

The results of a two-dimensional flexural analysis applied to the Andean margin, which is based on the correlation between topography and Bouguer anomaly, are here reviewed in order to characterize rigidity variations across and along the forearc–arc transition of the Central Andes and to understand the role of the forearc in the formation of the Altiplano Plateau. The forearc has maximum rigidities between 15° and 23°S. Forearc rigidity decreases gradually southward and sharply toward the plateau. The main orogen (elevations higher than 3000 m) is very weak along the entire Central Andes. A semi-quantitative interpretation of these trends, based on the relationship between flexural rigidity and the thermo-mechanically- and compositionally-controlled strength of the lithosphere, allows the following conclusions to be made: (1) across-strike rigidity variations are dominated by the thermal structure derived from the subduction process; (2) the forearc constitutes a strong, cold and rigid geotectonic element; (3) southward weakening of the forearc is directly related to the decreasing thermal age of the subducted slab; (4) very low rigidities along the main orogen are caused by the existence of a thick, quartz-rich crust with a low strain rate-to-heat flow ratio; (5) the strength of the plateau lithosphere is localized in an upper-crustal layer whose base at ~15 km could be correlated with a P-to-S seismic wave converter (TRAC1 of Yuan et al., 2000 [Yuan, X., Sobolev, S., Kind, R., Oncken, O. et al. 2000. Subduction and collision processes in the Central Andes constrained by converted seismic phases. *Nature*, V 408, 21/28 Diciembre, p. 958–961]); (6) the forearc–plateau rigidity boundary corresponds to a zone of changing thermal conditions, eastward-increasing crustal thickness and felsic component in the crust, and low strain-rate deformation, which correlates with a west-verging structural system at the surface. These conclusions suggest that the rigid forearc acts as a pseudo-indenter against the weak plateau and allows the accumulation of ductile crustal material that moves westward from the eastern foreland. This pseudo-indenter is geometrically represented by a crustal-scale triangular zone rooted at TRAC1. This model allows the integration of existing contradictory ideas on the dynamics of forearc–plateau interaction that are

* Tel.: +49 30 83870389.

E-mail address: andres@geophysik.fu-berlin.de.

related to the relative importance of upper-crustal compressive structures and lower crustal accumulation below the forearc.

© 2005 Elsevier B.V. All rights reserved.

Keywords: Elastic thickness; Rheology; Geotectonics; Forearc; Plateau; Andes

1. Introduction

The Andean Cordillera is the classic example of a mountain chain formed during the subduction of an oceanic slab under a continental plate. In this non-collisional geotectonic environment, the existence of the Altiplano–Puna Plateau (15°–28°S), the biggest continental plateau on the Earth after Tibet, is a highly intriguing phenomenon. As a result of the geoscientific work carried out in the last decades, it is now accepted that the huge crustal volume related to plateau formation (up to 75 km crustal thickness, Beck et al., 1996; Yuan et al., 2002) is principally due to crustal shortening concentrated at the eastern-most edge of the orogen during the Neogene (Allmendinger et al., 1997; Lamb and Hoke, 1997; Baby et al., 1997; Kley et al., 1999; McQuarrie, 2002). But a remaining question is how to relate this building mechanism at a lithospheric scale with the processes occurring at the western side of the orogen where the Nazca and South American plates are actually interacting. There are still no explicit answers to this question. Moreover, much of the work that discusses this topic expresses contradictory ideas, mainly about the relative geotectonic importance of upper-crustal compressive structures with respect to lower-crustal ductile deformation below the forearc (compare for example Isacks, 1988; Lamb and Hoke, 1997; Wörner et al., 2000 and Wörner and Seyfried, 2001 with Muñoz and Charrier, 1996; Victor et al., 2004 and García and Herail, 2001).

Based on the results of a flexural analysis applied to the Andean margin (Tassara, 1997; Tassara and Yañez, 1996, 2003), this review evaluates the mechanical state of the western slope of the Central Andean segment (15°–34°S) and contributes to a better understanding of the tectonic role of the forearc in the formation of the plateau. In contrast to other flexural approaches (e.g. Stewart and Watts, 1997), this analysis examines spatial variations of forearc

rigidity and along-strike gradients of horizontal stresses. The results are discussed from a rheological and tectonic point of view and allow a new geotectonic model of the slab–forearc–arc interaction to be proposed.

2. Geotectonic description of the Central Andes

The present-day Andes are principally the result of an orogenic process that started in the Late Oligocene after a major reorganization of the oceanic plates in the eastern Pacific (e.g. Tebbens and Cande, 1997). This reorganization produced a tripling of the convergence rate to 150 mm/year (Pardo-Casas and Molnar, 1987; Somoza, 1998). Since the Early Miocene, the convergence rate has diminished continuously to the current situation in which the Nazca and South American plates move at almost the same absolute rate of ~37 mm/year (at ~23°S), giving a total convergence of ~74 mm/year in the direction N78°E (Norambuena et al., 1998; Angermann et al., 1999).

The Central Andes (15°–34°S) are considered here to be a continental-scale segment of the Andean convergence system. The limits of this segment coincide with the boundaries of several morphotectonic units of the continental plate (see Fig. 1). These limits are also correlated with abrupt N–S changes from “flat” (<10° dip) to “normal” (~30° dip) subduction in the depth range 100 to 150 km, and with the intersection of the Nazca and Juan Fernández oceanic ridges with the continental margin. Based on along-strike variations of topography, volcanism, tectonic style and subduction conditions, the Central Andes can be divided into three second order segments, which are here named Altiplano (15°–23°S), Puna (23°–28°S) and Frontal Cordillera (28°–34°S). The definition and nomenclature of these segments are partially taken from Jordan et al.

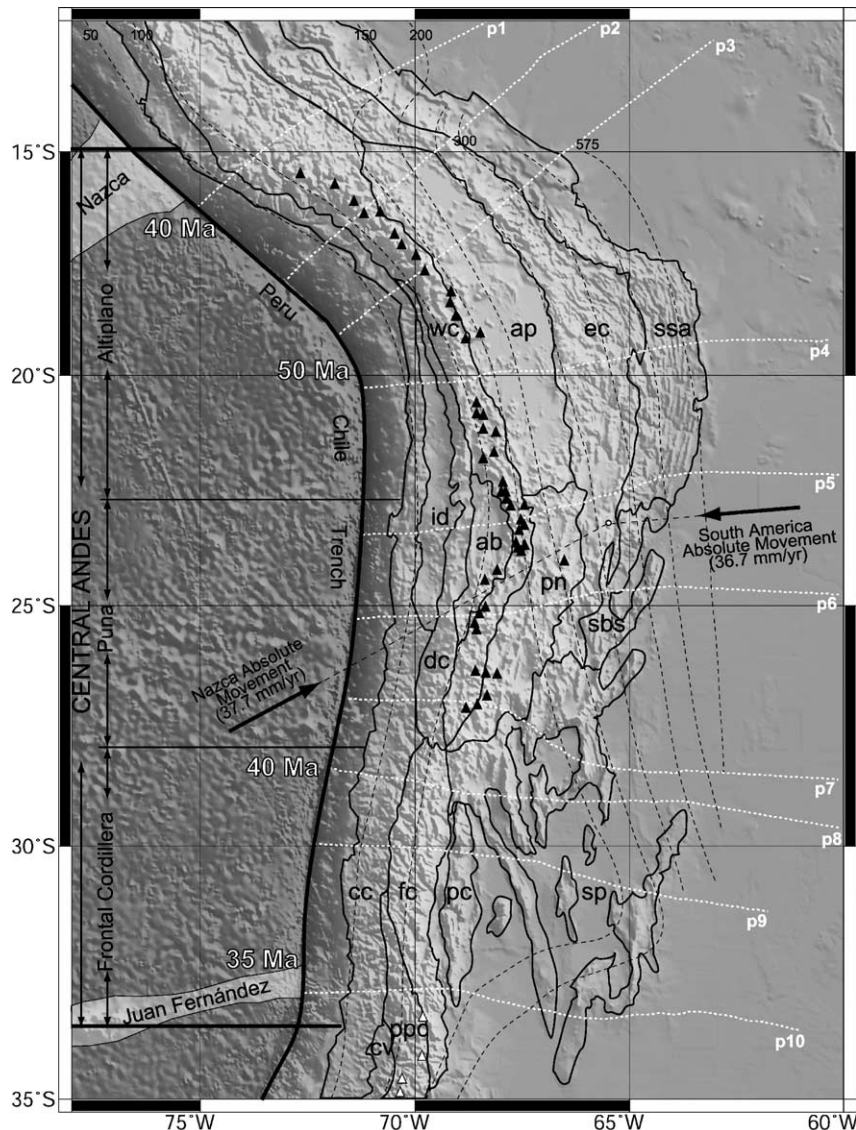


Fig. 1. Geotectonic framework of the Central Andean convergence system between 12° and 35°S on a grey-shaded image of topography and bathymetry (USGS, 1996; Smith and Sandwell, 1997). Morphotectonic units of the continental plate are depicted (partially modified from Mpodozis and Ramos, 1989): cc, Coastal Cordillera; id, Intermediate Depression; cv, Central Valley; dc, Domeyko Cordillera; wc, Western Cordillera; fc, Frontal Cordillera; ppc, Principal Cordillera; ab, Atacama Basin; ap, Altiplano; pn, Puna; pc, Precordillera; ec, Eastern Cordillera; sp, Sierras Pampeanas; ssa, Sierras Subandinas; sbs, Santa Barbara System. Triangles are active volcanoes of the Central (black) and Southern (white) Volcanic Zones. Dashed black lines are 50 km contour lines of the subducted oceanic plate (Cahill and Isacks, 1992). Nazca and South American absolute motion vectors with respect to a point in the Eastern Cordillera are from Marret and Strecker (2000). The position of the Nazca and Juan Fernández oceanic ridges, as well as ages of the Nazca plate at the trench (from Müller et al., 1997), are also shown. The Central Andes are subdivided into Altiplano, Puna and Frontal Cordillera segments (partially modified from Jordan et al., 1983; Mpodozis and Ramos, 1989; Kley et al., 1999). Profiles used in the flexural analysis are shown by the dashed white lines labelled p1 to p10.

(1983), Mpodozis and Ramos (1989) and Kley et al. (1999). Here the term “main orogen” is used to refer to the sector comprising elevations higher than 3000 m.

In the next sections, the forearc and main orogen-foreland sectors of the Central Andes are described separately.

2.1. Forearc

The Peru–Chile trench has a maximum depth of 8000 m. It is almost free of sediments and no accretionary prism is observed along the margin (e.g. von Huene et al., 1999). East of the trench, the oceanic Nazca plate subducts with a constant dip of 30°S (Cahill and Isacks, 1992; Creager et al., 1995) and the continental slope ascends steeply to the coast. The distance between the trench axis and the coast has a maximum of 170 km at the Arica bend (18°S) and a minimum of 70 km at 29°S. This geometry is correlated with the curvature of the margin: concave-seaward in the Altiplano segment (Bolivian Orocline of Isacks, 1988) and convex-seaward in the Frontal Cordillera segment. Eastward of the coast line and along the entire margin, uplifted metamorphic (Palaeozoic) and basic magmatic (Mesozoic) rocks of the Coastal Cordillera are exposed. Behind this unit, the Intermediate Depression basin is filled with Cenozoic volcanosedimentary deposits (Hartley et al., 2000). South of 26°S this basin disappears and the slope of the Coastal Cordillera ascends continuously to the crest of the Andes. No Neogene structural boundary between the forearc and the main orogen has been reported along the Frontal Cordillera segment. The Domeyko Cordillera (or Chilean Precordillera) at the eastern side of the Intermediate Depression, is an Eocene magmatic and tectonic belt exhuming late Palaeozoic felsic igneous rocks (Mpodozis and Ramos, 1989), which north of 25°S is related to a west-verging, high-angle structural system that propagated slowly to the west during the Neogene (Muñoz and Charrier, 1996; Victor et al., 2004; García et al., 2002; Jacay et al., 2002; Fariás et al., in press). This structural system has been described as the western tectonic limit of the Altiplano–Puna Plateau and following Muñoz and Charrier (1996) hereafter will be named the “West-vergent Thrust System” (WTS). Between 23° and 25°S, and to the east of the Domeyko Cordillera lies the Atacama basin, a major topographic and geologic anomaly that is one of several anomalous features occurring across the margin at this latitude (Schurr et al., 1999; Götze and Krause, 2002; Belmonte, 2002).

2.2. Main orogen and foreland

The Central Volcanic Zone (CVZ) of the Andes (15°–28°S) is a chain of Quaternary stratovolcanic

complexes and andesitic–rhyodacitic domes of high-K calcalkaline affinities (Allmendinger et al., 1997; Kay et al., 1999) located on top of the Western Cordillera (max. elevations >6000 m). This unit also contains exposures of well-preserved volcanic features of middle Miocene to Pliocene ages (Wörner et al., 2000). Along the Altiplano and Puna further east, there are restricted outcrops of shoshonitic basalts and several large silicic complexes (de Silva, 1989). The Altiplano is an internally drained basin filled with gently deformed Cenozoic synorogenic sediments and volcanics (Allmendinger et al., 1997; Baby et al., 1997; McQuarrie, 2002), located at a constant elevation of 3800 m. In contrast, the Puna further south has irregular elevations averaging 4200 m.

The eastern boundary of the Altiplano–Puna Plateau is the Eastern Cordillera (max. elevations >5000 m), a doubly-vergent deformation belt active until the middle–late Miocene (Heraul et al., 1996; McQuarrie, 2002). The active deformation of the Altiplano segment has been absorbed since late Miocene at the eastward-propagating thin-skinned belt of the Sierras Subandinas. The tectonic style of the active foreland deformation changes transitionally south of 23°S from the doubly-vergent thick-skinned Santa Barbara System toward the uplifted basement blocks of the Sierras Pampeanas south of 27°S. These elongated, narrow and 4000 m high ranges of crystalline Palaeozoic rocks extend up to 700 km to the east of the trench axis. They were uplifted synchronously with the thin-skinned deformation of the (Argentinean) Precordillera (Ramos et al., 2002).

The main orogen south of 28°S is occupied by the Frontal Cordillera. This unit could be considered, at least lithologically, a southward continuation of the Domeyko Cordillera. Described by Allmendinger et al. (1990) as a narrow plateau of 80 km width and average elevation of 4000 m (up to 6500 m), this cordillera was uplifted by a doubly-vergent basement fault system during the late Miocene. This uplift occurred synchronously with the final phase of thin-skinned deformation of Mesozoic sedimentary sequences belonging to the Principal Cordillera in the south-western part of the main orogen (Cristallini and Ramos, 2000; Ramos et al., 2002). These events correlate with the eastward shift and then cessation of the volcanic arc at the Sierras Pampeanas, which has been interpreted as an indication of the temporal

development of flat subduction (e.g. Gutscher et al., 2000; Kay and Mpodozis, 2002; Ramos et al., 2002).

3. Flexural analysis

3.1. Data

A two-dimensional flexural analysis was applied to 15 profiles between 15° and 47°S (Tassara, 1997; Tassara and Yañez, 1996, 2003). Ten of these profiles covering the Central Andes region are shown in Fig. 1 (p1 to p10). Each profile is orthogonal to the trench axis and extends eastward more than 1000 km into the stable South American craton. Data-spacing along profiles is 5 km and each point contains, as input data to the flexural analysis, bathymetry-topography and Bouguer anomaly. The former was interpolated from Smith and Sandwell (1997) and GTOPO30 (USGS, EROS data centre, 1996) digital datasets. Bouguer anomalies were extracted from a grid computed by SERNAGEOMIN (Chilean Geological Survey) that is based on more than 100 000 gravimetric stations compiled from different sources (see Tassara, 1997, for a full description).

3.2. Method

Fig. 2 summarizes the concepts behind the implemented method (see also Turcotte and Shubert, 1982; Watts, 2001). This flexural analysis assumes that the continental lithosphere is a two-dimensional thin elastic plate of variable thickness T_e overlying an inviscid asthenospheric mantle. This lithosphere is composed of a crust with density $\rho_c=2900 \text{ kg/m}^3$ and a lithospheric mantle with density $\rho_m=3300 \text{ kg/m}^3$. Flexural rigidity is defined as $D = \frac{E}{12(1-\nu^2)} T_e^3 \text{ [Nm]}$ (Turcotte and Shubert, 1982). Poisson Ratio ν and Young Modulus E are considered constants with magnitudes 0.25 and 70 GPa respectively. In this framework, across-strike variations in T_e (from trench to craton in this case) control the rigidity distribution of the lithosphere. Under the effect of vertical topographic loads $g\rho_c h(x)$ [with $g=9.8 \text{ ms}^{-2}$, $h(x)$ elevation] and total horizontal stresses σ_h (resulting from compressive external forces and tensional internal body force), the elastic lithosphere is deflected downward. This drives the deflection of

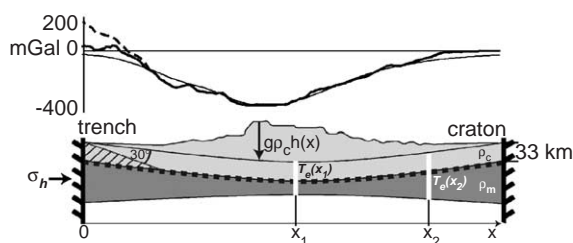


Fig. 2. Conceptual sketch of the applied flexural analysis. The continental lithosphere is a thin elastic plate, whose thickness T_e is allowed to change along the horizontal x -axis (note different values of T_e at x_1 and x_2). The lithosphere is composed of a crust of density $\rho_c=2900 \text{ kg/m}^3$ and 33 km thickness and a lithospheric mantle of density $\rho_m=3300 \text{ kg/m}^3$. Vertical topographic load $g\rho_c h(x)$ [$g=9.8 \text{ ms}^{-2}$, $h(x)$ topographic elevation] and total horizontal stress σ_h drive the downward deflection of the whole lithosphere and its embedded Moho (dotted line). The density contrast between crust and mantle (-400 kg/m^3) generates a long-wavelength Bouguer anomaly (thin line in upper part of the figure). The model lithosphere is fixed at both extremes of the profile, which implies zero deflection at the trench and easternmost craton. Replacement of dense oceanic lithosphere ($\rho=3100 \text{ kg/m}^3$) by continental crust at the westernmost edge of the modelled profile impose an artificial mass deficit that is subtracted from the observed Bouguer anomaly (dashed line in upper part of the figure) by computing the gravity effect of a triangular body of oceanic lithosphere (dashed area) below a subduction plane dipping 30° to the east. The corrected Bouguer anomaly (thick line in upper part of the figure) can be compared with the model-generated anomaly during an iterative change of $T_e(x)$ and σ_h that conclude with the best visual fit between observed and calculated anomalies at long wavelengths ($>300 \text{ km}$).

the embedded Moho and due to the density contrast between crust and mantle (here -400 kg/m^3), a long-wavelength Bouguer anomaly is generated.

A modified version of the finite difference code of Bodine (1981) was used to solve the equations associated with the flexural problem (see Tassara, 1997 and Tassara and Yañez, 2003, for a full description). According to the thin elastic plate approximation, this problem is restricted to one dimension (x in Fig. 2) and each profile is divided into elements of 5 km length. Both extremes of the profile are fixed (zero deflection at trench and easternmost craton), and an initially constant crustal thickness of 33 km was used.

The set-up imposes an artificial mass deficit (with respect to the real Earth) at the westernmost edge of the model. This is because the dense oceanic lithosphere below the subduction plane is replaced by continental crust in the starting model. In order to

realistically compare the Bouguer anomaly generated by the model with the observed anomaly along each profile, a correction was applied to the observed anomaly to account for this mass deficit. The subtracted correction along each profile is simply the gravity effect (relative to a continental crust of density 2900 kg/m^3) of a triangular body formed by

oceanic lithosphere (density= 3100 kg/m^3) below the slab top dipping at 30° to a depth of 33 km (dashed area in Fig. 2). The geometry of this body is consistent with the subduction geometry reported by Cahill and Isacks (1992; see Fig. 1) and allows the method to be applied continuously from the westernmost part of the forearc to the entire

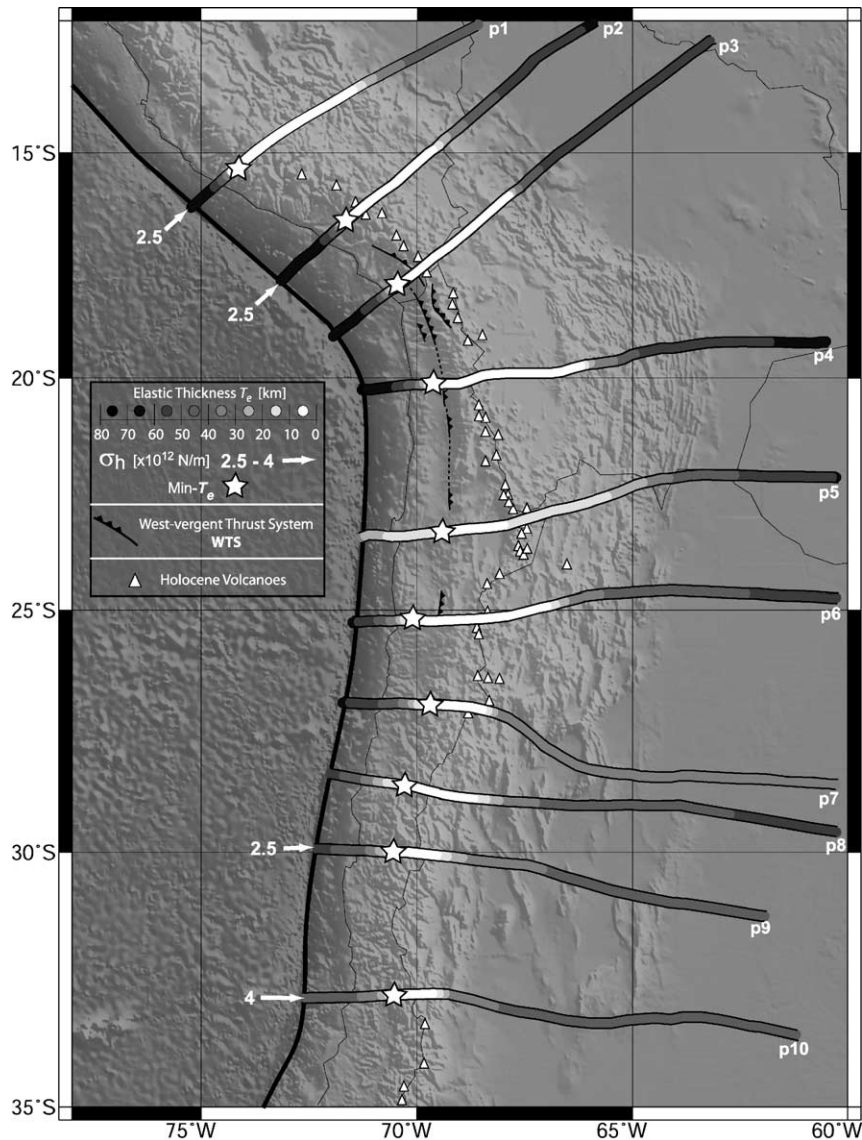


Fig. 3. Results of the applied flexural analysis. Values of elastic thickness T_e along each modelled profile are shown by grey tones between black for $T_e > 70 \text{ km}$ and white for $T_e < 10 \text{ km}$. A white star marks the position of the minimum T_e value (Min- T_e) along each profile. Arrows with values are the estimated total Horizontal Stress σ_h [$\times 10^{12} \text{ N/m}$] for profiles where it is not zero. Also shown are the Holocene volcanoes and the main structures of the “West-vergent Thrust System” (WTS, from Victor et al., 2004; García et al., 2002; Jacay et al., 2002).

continental margin. The long-wavelength “corrected” Bouguer anomaly is taken as the actual signal of the Moho and lithospheric deflection, a procedure supported by the small relative influence of sub-crustal sources in the Andean gravity field (Götze and Kirchner, 1997; Kösters, 1999).

An iterative change both in the elastic thickness structure along the profile $T_e(x)$ and the value of total horizontal stress σ_h , allows the best visual fit between corrected and model-generated Bouguer anomalies at long-wavelengths (>300 km) to be found. This exercise concludes with the final values of $T_e(x)$ and σ_h for each profile.

Sensitivity analyses (Tassara, 1997) indicate that elastic thickness variations of 20% produce changes in the predicted Bouguer anomaly that are within the ± 25 mGal error for observed anomalies. This gives an indication of the uncertainty associated with the method. Similarly, σ_h is estimated with a total uncertainty of $\pm 1.25 \times 10^{12}$ N/m.

3.3. Results

Final T_e estimates resulting from the modelling are presented in Fig. 3, together with σ_h values for those profiles where it is not zero. Along each modelled profile, T_e values are depicted by different grey tones and a white star marks the position of the minimum elastic thickness value (Min- T_e). Also shown are the Holocene volcanoes and main structures of the West-vergent Thrust System (WTS, after Victor et al., 2004; García et al., 2002; Jacay et al., 2002), that will be discussed in the next sections. Table 1 summarizes the most relevant parameters describing these results.

Fig. 4 shows “corrected”, model-generated and residual Bouguer anomalies of four representative profiles. For wavelengths comparable with the main orogen (>300 km), the residuals (or misfit) resulting from the model show values lower than ± 30 mGal. Observing Fig. 4 and considering that the Bouguer anomaly ranges between 200 and -450 mGal at these latitudes (e.g. Götze et al., 1994), these residuals represent less than 5% of the maximum variation of the gravimetric signal, thus supporting the validity of the results.

At shorter wavelengths and in accordance with the simple lithospheric model and boundary conditions imposed, higher residuals appear. In the forearc, residuals are on average 50 mGal. The existence of these residuals, added to the fact that values of T_e calculated at the trench axis represent a maximum estimate of the actual values that could exist there (due to the zero-deflection imposed at the trench) and considering the uncertainties induced by the method in T_e estimates, justifies the use of these results for a semi-quantitative evaluation of first-order, continental-scale rigidity variations across and along the continental margin.

From Fig. 3 and Table 1, the following first-order spatial trends of elastic thickness and horizontal stress can be delineated:

- Profile 5 (p5, 23°S) has anomalous values compared with profiles north and southward. This fact is related to the anomalous character of the whole lithosphere of the northern Puna segment, i.e. the presence of major morphological anomalies (e.g. Mejillones Peninsula and Salar de

Table 1
Values of relevant parameters estimated for each profile

Segment	Altiplano				Puna			Frontal Cordillera		
Profile (Lat.)	p1 (15°S)	p2 (17°S)	p3 (18°S)	p4 (20°S)	p5 (23°S)	p6 (25°S)	p7 (26.5°S)	p8 (28.5°S)	p9 (30°S)	p10 (33°S)
Min- T_e	5.5	4.5	5	1	7	4	0	0	2.5	3
Max- T_e	71	69	69	72	36	63	62	57	55	47
d	145	215	195	190	255	145	215	215	210	240
ΔT_e	0.45	0.30	0.33	0.37	0.11	0.41	0.29	0.27	0.25	0.18
σ_h [$\times 10^{12}$ N/m]	2.5	2.5	0	0	0	0	0	0	2.5	4
Variations	High rigidity of the forearc				Anomaly	Southward decrease of the forearc rigidity				

Min- T_e —Minimum value of elastic thickness; Max- T_e —Maximum value of elastic thickness at the trench; d —distance between Min- T_e and Max- T_e ; ΔT_e —gradient of elastic thickness—(Max- T_e –Min- T_e)/ d ; σ_h —total horizontal stress.

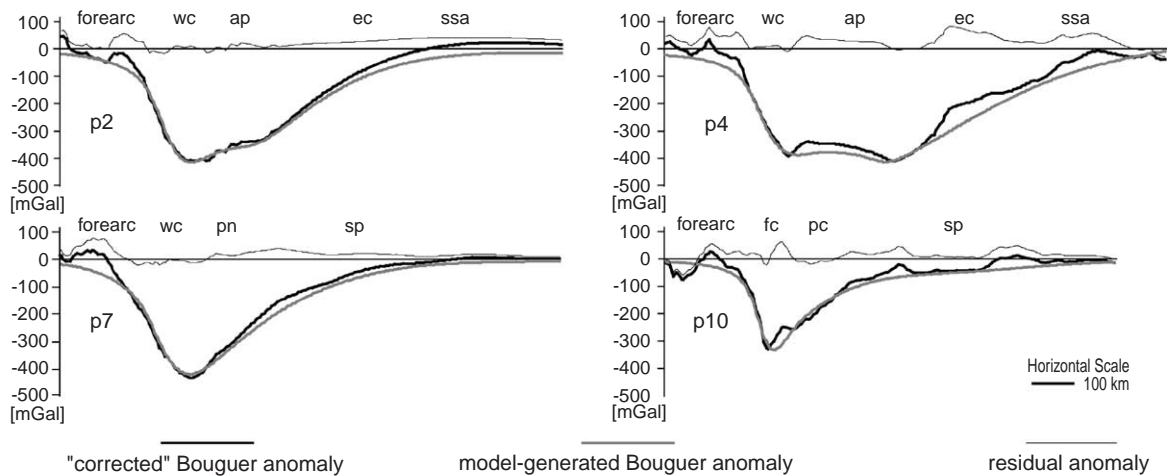


Fig. 4. “Corrected”, model-generated and residual (corrected—model-generated) Bouguer anomalies along four representative profiles (p2, p4, p7, p10). Note that at long wavelengths residuals are lower than ± 30 mGal. In the forearc they are of the order of 50 mGal. Morphotectonic units are as named in Fig. 1.

Atacama), anomalously thick crust in the forearc (e.g. Giese et al., 1999) and a postulated thermal mantle anomaly that at least partially compensates the Puna elevation (e.g. Withman et al., 1996). The existence of these anomalies makes it impossible to apply the above described assumptions and method to this sector. In the subsequent description and discussion, this profile will not be considered.

- For each profile, T_e shows maximum values ($\text{Max-}T_e$) at the trench axis. In the Altiplano segment, $\text{Max-}T_e$ varies between 69 km (p2–3) and 72 km (p4). South of 26°S , $\text{Max-}T_e$ diminishes systematically to 47 km at 33°S (p10).
- The minimum value of T_e ($\text{Min-}T_e$) along the Altiplano segment is located in the western part of the Domeyko Cordillera, in spatial correlation with the WTS. Further south, $\text{Min-}T_e$ is at the western limit of the Frontal Cordillera.
- T_e diminishes relatively sharply toward the main orogen. This decrease is depicted by the spatial gradient of T_e : $\Delta T_e = (\text{Max-}T_e - \text{Min-}T_e)/d$ (with d the distance between $\text{Max-}T_e$ and $\text{Min-}T_e$). ΔT_e has a maximum of 0.45 in the Altiplano–Puna segments (p1) and decreases gradually south of 26°S to a minimum of 0.18 at 33°S (p10).
- Along all the modelled profiles the main orogen is characterized by T_e values lower than 10 km. In

the Altiplano segment, this very low T_e zone extends up to the central part of the Eastern Cordillera and further south it includes the Argentinean Precordillera.

- East of the very low T_e zone, the elastic thickness increases to values in the range 65 km (Altiplano segment) to 45 km (Frontal Cordillera segment).
- Estimated σ_h , with an uncertainty of $\pm 1.25 \times 10^{12}$ N/m, is 2.5×10^{12} N/m between 15° and 17°S , zero between 18° and 29°S and then increases southward to values of 2.5×10^{12} N/m at 30°S and 4×10^{12} N/m at 33°S .

The decrease of both $\text{Max-}T_e$ and ΔT_e south of 26°S is interpreted as an indication of a real decrease in the forearc rigidity. It is also important to note the existence of a sharp rigidity contrast between the forearc and the main orogen of the Altiplano segment (as is shown in profiles p1 to p4).

4. Interpretation and discussion of the results

4.1. Basis for a geotectonic interpretation of T_e estimates

In order to give a sufficient framework for geotectonic interpretation of T_e variations across and along the Central Andes, the relationship between T_e

and parameters describing the rheology and structure of the continental lithosphere must be discussed. A full discussion of this topic can be found in Kuszniir and Karner (1985), Ranalli (1994), Burov and Diament (1995), Jackson (2002) and in Tassara (1997) and Tassara and Yañez (2003).

Let $\sigma(z)$ be defined as the deviatoric stress externally applied to a two-layer lithosphere (crust and mantle), and $\Gamma(z)$ as the internal yield strength of this lithosphere (both depending on depth z). If crust and mantle are mechanically coupled, T_e is equal to the depth range over which $\sigma(z) < \Gamma(z)$. Within this range, $\sigma(z)$ is elastically supported. Above and below this elastic beam, $\sigma(z)$ generates permanent deformation of brittle and ductile nature, respectively. Brittle strength is commonly described by Byerlee's law (Byerlee, 1978), which depends only on the brittle gradient and increases linearly with depth. Ductile strength is non-linearly dependent on strain rate, temperature and rock type (e.g. Carter and Tsenn, 1987).

According to the definition of the elastic thickness and for a given external stress field and brittle gradient, T_e is determined by the ductile strength of the lithosphere and thus is also dependent on the intrinsic crustal and mantle lithologies and on the extrinsic thermo-mechanical regime defined by strain rate $\dot{\epsilon}$ and temperature distribution. In a first approximation this distribution can be described by a linear geothermal gradient that depends only in the thermal conductivity and the surface heat flow density Q , a parameter that can be measured on the Earth surface. An inspection of the commonly advocated law of ductile dislocation-diffusion creep of polymineralic materials (e.g. Carter and Tsenn, 1987; Ranalli, 1987; Burov and Diament, 1995; Porth, 2000) allows the conclusion that T_e is an increasing function of the strain rate-to-heat flow ratio $\dot{\epsilon}/Q$ acting on the lithosphere, though it is more sensitive to changes in Q due to the exponential relationship between temperature and ductile strength. Moreover, it is accepted that the strength of a polymineralic material is dominated by the absolute content of quartz, which is the weakest mineral in a silicate assemblage (e.g. Carter and Tsenn, 1987; Handy, 1990; Burov and Diament, 1995). Thus, different crustal rheologies should be described by the content of this mineral in the crust and, in this way, it can be established that

ductile strength and T_e are a decreasing function of this quartz content.

Mantle rheology is commonly described by the properties of wet dunite (Carter and Tsenn, 1987; Burov and Diament, 1995; Porth, 2000), and reductions in its strength derive mostly from water content, a factor that also plays a role in crustal strength (e.g. Jackson, 2002). Finally, if crust and mantle are mechanically decoupled by a ductile lower crust, T_e is strongly reduced and the amount of reduction increases with increasing crustal thickness (Burov and Diament, 1995; Porth, 2000).

In summary: for a given external deviatoric stress field, an assumed value of brittle gradient and a homogeneous wet dunite mantle, T_e is an increasing function of the strain rate-to-heat flow ratio $\dot{\epsilon}/Q$ and a decreasing function of the thickness and quartz content of the crust. In the next sections, this relationship is used to discuss selected aspects of the rigidity distribution estimated by the flexural analysis.

4.2. Across-strike T_e variations

Fig. 5 presents T_e profile p4 at 20°S together with the 2D steady-state thermal structure calculated at 21°S by Springer (1999) assuming a subduction model for forearc and magmatic arc and a crustal stacking model describing simple underthrusting for the eastern Plateau and foreland. The comparison between model-derived surface heat flow density Q and the averaged measurements at each morphotectonic unit reported by Springer and Förster (1998) are also shown, as are topography and the Moho discontinuity at 20°S after Yuan et al. (2000). There is a clear correlation of T_e with the isotherm-path that suggests that the subduction-derived thermal structure controls the global rigidity of the continental lithosphere. This conclusion can be extended to the whole margin if it is assumed that thermal models of subduction zones, independent of subduction parameters, show always the general structure described by Springer (cf. Peacock, 1996; Gutscher et al., 2000).

The subducted slab thermal control on continental rigidity seems to be especially relevant at the cold and rigid forearc where a conduction-dominated thermal model successfully reproduces the low Q values reported here. However, Springer's model is not able to explain high Q values at the Plateau (locally as high

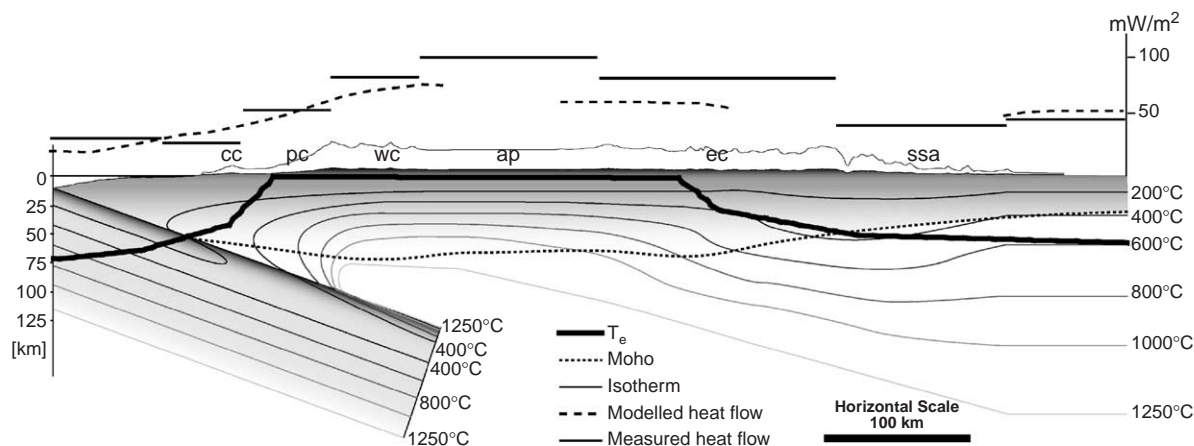


Fig. 5. Across-strike section at 20°S showing the modelled T_e profile p4 (thick solid line), isotherms after Springer (1999), Moho discontinuity (dotted line) after Yuan et al. (2000), surface heat flow density derived from the Springer's model (dashed line) and average heat flow density measured by Springer and Förster (1998) (straight lines). Topography is exaggerated five times and morphotectonic units are as named in Fig. 1.

as 180 mW/m²). According to Babeyko et al. (2002), this discrepancy can be explained by assuming thermal convection of a felsic, ductile and hot lower crust together with the existence of shallow magma chambers. The sharp change from high T_e at the forearc to very low T_e at the main orogen could be interpreted in terms of this across-strike change of the thermal regime. However, the position of Min- T_e to the west of the volcanic arc and its related thermal anomaly (see Figs. 3 and 5) suggests that other factors, like the increase of crustal thickness toward the orogen, across-strike changes of crustal lithology from mafic-dominated at the forearc to felsic-dominated at the Plateau (e.g. Lucassen et al., 2001) and the injection of slab-derived water into the lithosphere below the Domeyko Cordillera (ANCORP, 1999; Giese et al., 1999), also control the localization of this rigidity boundary.

Low T_e values west of the main orogen could partially be caused by faulting and low strain rates. This suggestion is supported by the spatial correlation between Min- T_e and the western limit of the West-vergent Thrust System (WTS). Estimates of deformation rates across the WTS (Victor et al., 2004) are as low as $5 \times 10^{-17} \text{ s}^{-1}$, a value that lies at the lower bound of geological strain rates (Pfiffner and Ramsay, 1982). Low deformation rates at the retro-wedge boundary of asymmetric, Altiplano-like plateaus have also been observed in numerical experiments conducted by Vietor and Oncken (2002).

4.3. North–south weakening of the forearc

South of the Altiplano segment, an along-strike weakening of the forearc can be observed (Fig. 3 and Table 1): Max- T_e =72 km and ΔT_e =0.37 at 20°S (p4) decrease to Max- T_e =47 km and ΔT_e =0.18 at 33°S (p10). This weakening is correlated with a decrease of the slab age from 50 Ma at 20°S to 35 Ma at 33.5°S (Fig. 1; Müller et al., 1997). According to the inverse relationship between thermal age and surface heat flow density for oceanic plates discussed by Turcotte and Shubert (1982, p. 165), such a north–south decrease of the slab age implies a ~20% increase in the slab-derived heat flow. Taking into account that T_e is a decreasing function of Q , this variation may explain the southward weakening of the forearc.

Tassara (1997) and Tassara and Yañez (2003) show that profile 10 at 33°S presents the minimum values of Max- T_e and ΔT_e found between 15° and 47°S. South of 33°S, these values are slightly higher (Max- T_e ≈ 50 km) than at this latitude, but still lower than along the Altiplano segment. The substantial forearc weakening observed at 33°S could be at least partially related to the thermal rejuvenation of the oceanic plate during its passage over the Juan Fernández hotspot. From forward modelling of magnetic anomalies, Yañez et al. (2001) point out that the age of the volcanic edifices forming the Juan Fernández ridge near the trench axis at 33°S is 9–10 Ma. Thus, this locally

young and hot oceanic lithosphere could generate a local maximum in the forearc weakening.

Another factor that seems to be coupled with these phenomena is the flattening of the subducted slab along the Puna and Frontal Cordillera segments. Although the change in slab dip angle occurs below 100 km depth and thus further east of the forearc domain (see Fig. 1), this flattening is associated with a southward increase of: the mechanical coupling in the Wadati-Benioff zone (Gutscher et al., 2000; Yañez et al., 2002), the maximum depth of the seismogenic zone (Klotz et al., 2001) and the liberated seismic energy (Gutscher, 2002; Pardo et al., 2002a). This southward increasing seismic activity along the interplate contact of the Frontal Cordillera segment could produce a high frictional heating that can also account for part of the southward weakening of the forearc.

The fact that a reduction of $\text{Max-}T_c$ and ΔT_c is not observed to the north of 20°S, in spite of decreasing slab age to 40 Ma at 15°S, suggests that both the local thermal anomaly associated with the Juan Fernández ridge and high frictional heating induced by flat subduction should be added to the main thermal control on forearc rigidity exerted by the slab age. These combined effects explain the along-strike variations of elastic thickness estimates.

4.4. Very weak main orogen

According to the concepts highlighted in Section 4.1 and following published analyses of 1D yield strength envelopes (Carter and Tsenn, 1987; Burov and Diament, 1995; Porth, 2000; Jackson, 2002; Tassara and Yañez, 2003), the very low values of elastic thickness along the whole main orogen of the Central Andes ($T_c < 10$ km; compare with values in Tables 5.2 and 6.2 of Watts, 2001), can be interpreted as the combined result of a thick and very weak crust dominated by a high quartz content and a low $\dot{\epsilon}/Q$ ratio.

Seismic experiments in the Altiplano and Puna segments suggest a Moho depth up to 75 km below the plateau and low seismic velocities and Poisson ratios (Zandt et al., 1994; Beck et al., 1996; Schurr et al., 1999; Swenson et al., 2000; Yuan et al., 2000, 2002). These low values have been interpreted to suggest that the crust is wholly felsic in composition

(e.g. Swenson et al., 2000; Yuan et al., 2002; Beck and Zandt, 2002). This interpretation is supported by the bulk felsic geochemical composition derived for the basement of these segments by Lucassen et al. (2001). South of 28°S, preliminary results of a seismic tomography study (Pardo et al., 2002b) indicate a Moho depth below the Frontal Cordillera of up to 70 km. According to Mpodozis and Kay (1990), late Palaeozoic felsic magmatic rocks that form the Frontal Cordillera are partially derived from an enriched felsic-like deep crustal source. All the preceding arguments support the existence of a relatively homogeneous, thick and quartz-rich crust that characterizes the main orogen of the entire Central Andes.

The existence of a low $\dot{\epsilon}/Q$ ratio along the Altiplano–Puna Plateau is directly supported by anomalously high Q values (up to 180 mW/m²; Henry and Pollack, 1988; Hamza and Muñoz, 1996; Springer and Förster, 1998). Strain rates calculated from geological deformation rates averaged over 10 Ma (Lamb, 2000; Hindle et al., 2002) and from non-seismic GPS velocities (Klotz et al., 2001; Bevis et al., 2001) are in the order of 10^{-15} s⁻¹ (intermediate range of geological strain rates, Pfiffner and Ramsay, 1982).

No heat flow measurements exist along the Frontal Cordillera, but Hamza and Muñoz (1996) suppose that this value should be in the order of 60 mW/m². This estimate is based on the maximum value observed north of 15°S by Henry and Pollack (1988) in a sector which is similar to the Frontal Cordillera segment in the sense that it has flat subduction and a related volcanic gap. In this context, the very low T_c estimated for the Frontal Cordillera segment can be explained only if the strain rate here is also very low. Considering the kinematic data of Giambiagi and Ramos (2002), Cristallini and Ramos (2000), Vergés et al. (2002) and Jordan and Allmendinger (1986) and then that the active deformation across this segment is taking place in a broad sector between the Frontal Cordillera (Cristallini and Ramos, 2000) and the eastern Sierras Pampeanas (Ramos et al., 2002), geological deformation rates averaged over 10 Ma can be estimated to lie in the range 10^{-16} – 10^{-17} s⁻¹. GPS velocities determined by Klotz et al. (2001) are in the order of 10^{-16} s⁻¹. A detailed discussion of this topic is beyond the scope of this contribution, but this thermo-mechanical change along the Central Andean

orogen, in the presence of a homogeneous thick and felsic crust, should be considered a key characteristic of the Andean system related to along-strike changes of the foreland tectonic styles and, from a geodynamic point of view, to the evolution of upper-plate deformation and synchronous flattening of the subducted slab.

1D yield strength envelopes (Carter and Tsenn, 1987; Burov and Diament, 1995; Porth, 2000; Jackson, 2002; Tassara and Yañez, 2003), also show that very low T_e values are an indication that the only sector of the lithosphere containing strength is the upper crust. For $T_e \approx 10$ km and depending on the assumed crustal rheology, the brittle–ductile transition should exist at a depth of 2–7 km. Below ~ 15 km, the lithosphere would have no strength and deform ductilely for all ranges of external forces. The proposed base of the competent upper crust at ~ 15 km depth correlates remarkably well with the position of a P-to-S seismic wave converter observed by Yuan et al. (2000) across the whole Plateau (trans-Andean converter one or TRAC1). This intra-crustal discontinuity is the top of a low velocity zone related to a high temperature zone with partial melting extending to middle-lower crustal depths (Yuan et al., 2000). This zone is also imaged as a high conductivity anomaly by magnetotelluric experiments (e.g. Brasse et al., 2002).

4.5. Estimates of horizontal stress σ_h

In the context of the mechanical model used in this study, estimates of horizontal stress σ_h should be interpreted as the sum of all horizontal stresses acting along the modelled profile. According to Froidevaux and Isacks (1984), Porth (2000) and Vanderhaeghe et al. (2003), horizontal stresses operating on a convergent continental margin derive mainly from the compressive force imposed by the convergence and the extensional body forces related to the gravitational relaxation of the orogen. Thus, along-strike variations of σ_h should reflect the combined effect of independent variations of both forces.

Values of $\sigma_h = 0 \pm 1.25 \times 10^{12}$ N/m observed between 18° and 28° S can be interpreted in terms of an almost neutral state of total horizontal stress along the Altiplano–Puna plateau. This neutral state results from cancellation of compressive forces exerted by

the convergence and extensional body forces related to the huge crustal root below the plateau. Allmendinger et al. (1997) point out that the current state of stress observed from seismic and neotectonic data in the central part of the Altiplano–Puna is neutral to extensional and suggest that “far field compression is balanced with the weight of the uplifted plateau”. The same observation is used by Froidevaux and Isacks (1984) to calculate an external compressive stress of 6.1×10^{12} N/m that balances the horizontal extensional stresses produced by the high and thick plateau. This value will be taken in the following discussion as the reference compressive stress that is imposed by the current convergence conditions along the Altiplano–Puna segment in order to neutralize the extensional stresses induced by the Plateau.

One of these convergence conditions is that the oceanic slab is older than 40 Ma (Fig. 1). The increase of σ_h north of 18° S to 2.5×10^{12} N/m and mainly south of 28° S to 4×10^{12} N/m (both with an uncertainty of $\pm 1.25 \times 10^{12}$ N/m) seems to be correlated with decreasing age of the Nazca plate at the trench (see Figs. 1 and 3). This decrease should cause an increment in the slab buoyancy that is locally reinforced around 15° S and 33.5° S by subduction of the Nazca and Juan Fernández buoyant oceanic ridges. Thus, values of $\sigma_h > 0$ can be interpreted as the expression of a high compressive stress, whose excess with respect to the horizontal extensional stress of 6.1×10^{12} N/m is due to the relatively high buoyancy of the subducted slab. In this context, the external compressive stress directly generated by the convergence ($\sigma_h + 6 \times 10^{12}$ N/m) can reach values of 8.5×10^{12} N/m and 10^{13} N/m at the northern and southern boundaries of the Central Andes. These values are slightly lower than typical slab pull stresses (e.g. Turcotte and Shubert, 1982, p. 287).

Along the Frontal Cordillera segment, two other phenomena can also account for the southward increase of σ_h . First, the previously discussed southward-increasing magnitude and depth of interplate coupling that is associated with the flattening of the subducted slab (see Section 4.3) allows the interpretation that the imposed compressive stresses are more efficiently transmitted to the continental lithosphere in this segment than further north. Second, the southward narrowing of the main orogen means a decrease of its total crustal volume and a corresponding

decrease in extensional body forces. Even if no increase of the external compressive stress is considered, this must generate a southward increase of the total horizontal stress (i.e. $\sigma_h > 0$). This reduction in extensional body forces also means that the compressive stress produced by the convergence at the southernmost limit of the Central Andes should be lower than 10^{13} N/m.

5. Geotectonic model of forearc–plateau interaction at the Altiplano segment

The results discussed in this paper indicate that the Andean forearc is a rigid geotectonic element on the western edge of the convergence system that is thermo-mechanically connected at long time-scales with the strong and cold subducted slab. Palaeomagnetic data on early Miocene rocks belonging to the Altiplano forearc (e.g. Roperch et al., 2000; Lamb, 2001; Arriagada et al., 2003) show no tectonic rotations during the Neogene. This suggests that the current curvature of the Bolivian orocline was acquired and frozen prior to the main phase of Plateau formation and that the high rigidity of the forearc could be traced as a long-term (at least 20 Myr) stable feature of the continental margin. The current subduction geometry along the Altiplano segment, which is dominated by the parallelism between the convergence vector and the symmetry axis of the Bolivian orocline (Gephart, 1994), probably is the steady-state situation in terms of the thermal control of the slab on the forearc rigidity.

In this context and in spite of the effective ~85% of convergence absorbed along the subduction plane (e.g. Klotz et al., 2001; Bevis et al., 2001), the long-term slab–forearc system can be interpreted as a rigid, indenter-like backstop that has resisted the westward movement of crustal material coming from the shortened eastern foreland. This material is thus forced to accumulate below the competent upper crust of the Altiplano.

Considering that the trench axis and forearc also move westward in an absolute reference frame, but with a rate ~30% slower than the stable South American craton (Lamb, 2000; Klotz et al., 2001; Bevis et al., 2001; Hindle et al., 2002), the slab–forearc system cannot be considered a real indenter in the sense of directly pushing toward the orogen and

producing the deformation and crustal thickening responsible for plateau formation (as is the case where India indents against Asia to produce the Tibetan Plateau; e.g. Tapponnier et al., 1986; Houseman and England, 1993).

Fig. 6 shows the proposed geometry for the convergence system and emphasises the structure forming the forearc–plateau transition. The upper eastern boundary of the forearc pseudo-indenter is marked by the downward extension of the WTS, the geometry of which was determined by Victor et al. (2004) from geometric modelling and restoration of surface structures at 20°23'S. The lower eastern boundary is here assumed to correspond with the path of the 350°C isotherm of Springer (1999), which limits the crustal seismicity observed in the forearc at 20°–22°S (ANCORP, 1999). This situation is also described at 22°–24°S by Belmonte (2002), who points out that the 350°C isotherm constitutes a cut-off limit for crustal seismicity and is therefore an important mechanical and rheological limit across the forearc–arc transition. David et al. (2002) also observe crustal seismicity concentrated in a west-dipping plane below the forearc at 18°–19°30'S, which they consider to be a “thermal and rheological boundary between the rigid forearc and the soft crust of the magmatic arc”. They calculate a stress tensor with a maximum compressive stress axis parallel to the convergence direction and dipping parallel to the west-dipping seismicity plane. This fact allowed them to propose the existence of a true east-verging compressive structure limiting the rigid forearc (Farias et al., in press). In the geometrical model proposed here, both boundaries define a crustal-scale triangular zone (Fig. 6). The eastern tip of this triangular zone is located 25 km below the Western Cordillera and is rooted at TRAC1 of Yuan et al. (2000). The spatial continuity of these three features along the Altiplano segment permits the proposed geometry to be extended to the entire margin between 18° and 23°S.

TRAC1 is here interpreted as the base of the competent upper crust of the plateau, which is thus decoupled from the westward-moving ductile crust related to the underthrusting of the Brazilian shield below the Sierras Subandinas (Fig. 6; see also Beck and Zandt, 2002). The proposed geometry below the Plateau and foreland is similar to the model of

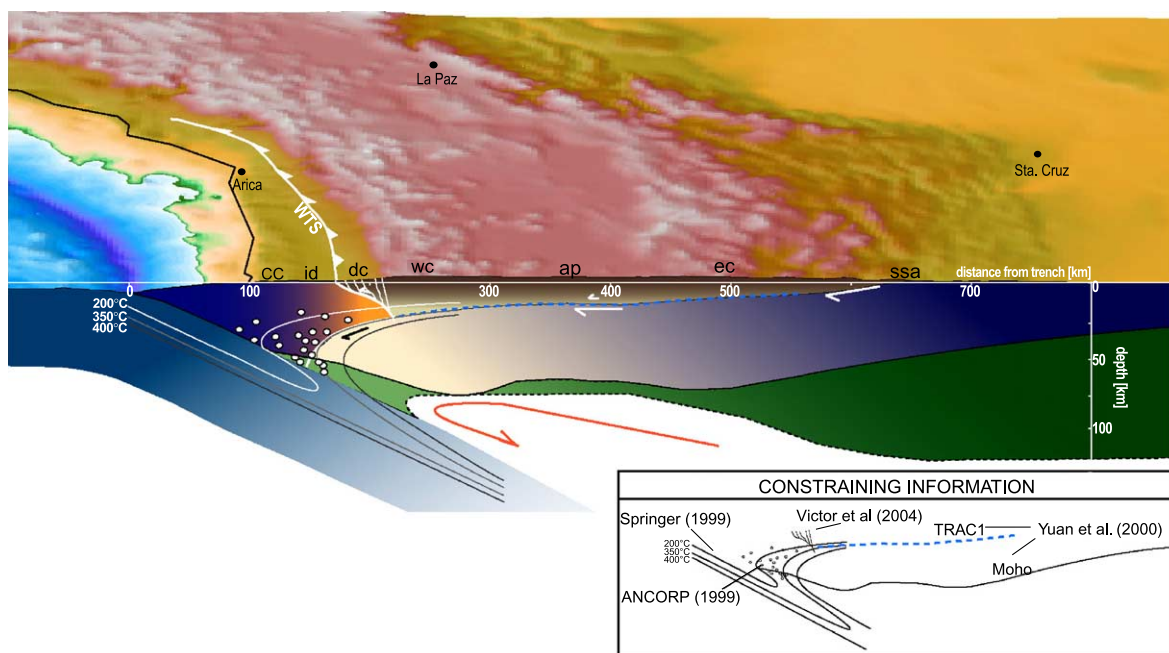


Fig. 6. Schematic cross-section at 20°S and a 3D view of topography and bathymetry along the Altiplano segment, presenting the proposed geometry of the forearc-plateau transition. Constraining information for this model is referred in the inset diagram. Dark grey tones represent rigid sectors (forearc, plateau upper crust and foreland) and light grey tones show weak crust (middle-lower plateau crust, forearc wedge). In the electronic version of this figure, dark blue colours in the continental crust represent rigid sectors (forearc and foreland), light red colours represent weak middle-lower crust, brown is the competent upper crust of the plateau, light blue is the oceanic plate and green is the lithospheric mantle. Crustal material in orange is confined to deform under low strain rates. Arrows depict the flow of material from the east.

McQuarrie (2002), who suggests that the existence and propagation of thin (15 km) and long (300 km) rigid basement sheets decoupled from lower crust are the principal mechanism of crustal shortening and thickening to form the Plateau. Here it is proposed that some sort of basal drag exists along TRAC1 which transfers to the competent upper crust a slow westward movement. This movement is related to the development of the WTS and its low deformation rates. The crustal material confined in the wedge of the forearc triangular zone should be subjected to high pressures and is probably deformed under low strain rates.

The ductile and partially melted middle-lower crust coming from the east is forced to circulate below the lower eastern boundary of the forearc. This process seems to be partially coherent with the mechanism proposed by Isacks (1988) to explain the formation of the western monoclinical flexure and subsequent westward tilting of the forearc during his simple-shear stage of Plateau uplift (late Miocene to present). In this scenario, the forearc and western orogen respond

passively to the uplift of the plateau as a single unit. A similar model has also been invoked by Lamb and Hoke (1997), Hartley et al. (2000) and Wörner et al. (2002), but all these authors do not consider or give little importance to the well-documented existence of west-verging, high-angle and high-throw structures uplifting the western margin of the Plateau (Muñoz and Charrier, 1996; Victor et al., 2004; García et al., 2002; Farías et al., *in press*). The geotectonic model proposed here allows the integration of these apparently contradictory ideas through the decoupling of upper and lower crustal deformation across a crustal-scale triangular zone linked with the forearc-plateau transition.

6. Conclusions

1. Review of a flexural analysis applied to the Central Andean margin (15°–34°S) shows the following results concerning forearc-arc interaction:

- a. The forearc region has high rigidity ($\text{Max-}T_e > 50$ km) decreasing relatively sharply toward the main orogen ($\Delta T_e > 0.18$), which itself is characteristically very weak ($T_e < 10$ km).
 - b. Both $\text{Max-}T_e$ and ΔT_e are maximum along the Altiplano segment and they decrease systematically southward. This is interpreted to reflect a southward weakening of the forearc.
 - c. The position of $\text{Min-}T_e$ along the Altiplano segment is correlated with the western limit of the Domeyko Cordillera and the “West-vergent Thrust System” (WTS) of Muñoz and Charrier (1996).
 - d. The total horizontal stress σ_h resulting from external compressive forces and internal gravitational forces is 2.5×10^{12} N/m between 15° and 17°S , zero between 18° and 29°S , and increases gradually southward up to values of 2.5×10^{12} N/m at 30°S and 4×10^{12} N/m at 33°S .
2. These results were interpreted and discussed from a rheological point of view through a relationship indicating that T_e is a decreasing function of crustal thickness and intrinsic quartz content in the crust and an increasing function of the extrinsic strain rate-to-heat flow ratio. The conclusions of this exercise are:
- a. Across-strike T_e variations are at first-order due to the thermal structure derived from the subduction process.
 - b. A sharp rigidity boundary across the Altiplano segment is caused by a combination of (1) a change from slab conduction-dominated thermal regime at the forearc to crustal thermal convection below the plateau (e.g. Babeyko et al., 2002); (2) an eastward increase of crustal thickness and water in the lithosphere; (3) an increasingly felsic crustal composition (e.g. Lucassen et al., 2001); (4) the existence of low strain rates below the Domeyko Cordillera (Victor et al., 2004).
 - c. North–south weakening of the forearc could be primary related to the decreasing thermal age of the Nazca slab below the continent. Other factors partially responsible for this weakening can be an increased frictional heating driven by the southward flattening of the subducted slab and a local thermal anomaly in the Nazca plate at 33°S related to the young and hot Juan Fernández ridge.
 - d. The forearc is a cold and rigid geotectonic element at the western edge of the continent that is thermo-mechanically controlled at long time-scales by the subducted slab. Absence of post-Oligocene vertical rotations in the Altiplano forearc (e.g. Arriagada et al., 2003) suggests that this rigid behaviour has existed throughout the evolution of the plateau.
 - e. Along the whole main orogen, $T_e < 10$ km reflects the existence of a thick, quartz-rich crust submitted to a low strain rate-to-heat flow ratio $\dot{\epsilon}/Q$. Geoscientific information supports such a characterization and the supposed low Q along the Frontal Cordillera segment (Hamza and Muñoz, 1996) implies a very low $\dot{\epsilon}$. This along-strike thermo-mechanical change along the axis of the main orogen is a key feature of the Andean orogeny.
 - f. According to yield strength envelopes, $T_e < 10$ km implies the existence of a competent upper crust whose base is located at 15 km depth. This depth is well correlated with the seismically-defined TRAC1 intra-crustal discontinuity (Yuan et al., 2000).
 - g. Estimates of total horizontal stress $\sigma_h = 0$ ($\pm 1.25 \times 10^{12}$ N/m) indicate a neutral stress state along the Altiplano–Puna plateau. Extreme values of 2.5×10^{12} N/m and 4×10^{12} N/m at the northern and southern boundaries of the Central Andes can be correlated with a high interplate coupling related to the high buoyancy of slabs younger than 40 Ma subducting together with oceanic ridges. Along the Frontal Cordillera, the southward increase of σ_h should be also caused by the narrowing of the thickened crust and the subsequent decrease of the extensional gravity forces related to the orogen.

The cold and rigid forearc of the Altiplano segment constitutes a pseudo-indenter which does not push but resists the relative motion of the ductile crustal material transported from the shortened eastern foreland. This material is forced to accumulate below the competent upper crust of the plateau. This pseudo-indenting forearc is shaped by the downward prolongation of the WTS, as is reported by Victor et al. (2004), and by the 350°C isotherm of Springer (1999) that limits reported crustal

seismicity (ANCORP, 1999). Both boundaries form a crustal-scale triangular zone whose edge is rooted at the TRAC1 seismic converter (Yuan et al., 2000). This discontinuity decouples an almost stationary (relative to the forearc) competent upper crust from a westward-moving, ductile middle-lower crust derived from the underthrusting of the Brazilian shield below the Sierras Subandinas. Basal drag along TRAC1 could transfer a slow westward movement to the upper crust of the plateau that is consistent with the low deformation rates of the WTS (Victor et al., 2004). This model reconciles contradictory ideas related to the importance of upper-crustal compressive structures relative to lower-crustal accumulation below the forearc in the dynamics of forearc–plateau interaction.

Acknowledgements

This work was initially carried out for my Masters Thesis at the Geology Department of the Universidad de Chile with supervision from Gonzalo Yañez. The work was conducted in close collaboration with the Geophysics Group of SERNAGEOMIN (Chilean Geological Service) and as part of the Chilean Fondecyt project 1930164. I am grateful to Hans-Jürgen Götze and Ron Hackney of Freie Universität Berlin for their suggestions and corrections that improved this paper. I appreciate the reviews and comments of Muriel Gerbault, Evgene Burov and Joseph Martinod. Some of the figures were made with GMT (Wessel and Smith, 1998). The publication of this contribution is supported by the German project SFB 267 “Deformation Processes in the Andes” of the Deutsche Forschungsgemeinschaft.

References

- Allmendinger, R.W., Figueroa, D., Snyder, D., Beer, J., Mpodozis, C., Isacks, B.L., 1990. Foreland shortening and crustal balancing in the Andes at 30°S latitude. *Tectonics* 9 (4), 789–809.
- Allmendinger, R., Jordan, T., Kay, S., Isacks, B., 1997. The evolution of the Altiplano–Puna plateau of the Central Andes. *Annual Reviews on Earth and Planetary Sciences* 25, 139–174.
- ANCORP Working Group, 1999. Seismic reflection image of Andean subduction zone revealing offset of intermediate depth seismicity into oceanic mantle. *Nature* 397, 341–344.
- Angermann, D., Klotz, J., Reiber, C., 1999. Space-geodetic estimation of the Nazca–South American Euler vector. *Earth and Planetary Science Letters* 171, 329–334.
- Arriagada, C., Roperch, P., Mpodozis, C., Dupont-Nivet, G., Cobbold, P.R., Chauvin, A., Cortés, J., 2003. Paleogene clockwise tectonic rotations in the forearc of central Andes, Antofagasta region, northern Chile. *Journal of Geophysical Research* 108 (B1), 2032, doi:10.1029/2001JB001598.
- Babeyko, A., Sobolev, S., Trumbull, R., Oncken, O., Lavier, L., 2002. Numerical models of curstal scale convection and partial melting beneath the Altiplano–Puna plateau. *Earth and Planetary Science Letters* 199, 373–388.
- Baby, P., Rochat, P., Mascle, G., Herail, G., 1997. Neogene shortening contribution to crustal thickening in the back arc of the Central Andes. *Geology* 25 (10), 883–886.
- Beck, S., Zandt, G., 2002. The nature of orogenic crust in the central Andes. *Journal of Geophysical Research* 107 (B10), 2230, doi:10.1029/2000JB000124.
- Beck, S., Zandt, G., Myers, S., Wallace, T., Silver, R., Drake, L., 1996. Crustal-thickness variations in the central Andes. *Geology* 24, 407–410.
- Belmonte, A., 2002. Krustale Seismizität, Struktur und Rheologie der Oberplatte zwischen der Präkordillere und dem magmatischen Bogen in Nordchile (22°–24°S). PhD thesis, Freie Universität Berlin, Germany.
- Bevis, M., Kendrick, E., Smalley Jr., R., Brooks, B.A., Allmendinger, R.W., Isacks, B.L., 2001. On the strength of interplate coupling and the rate of back arc convergence in the central Andes: an analysis of the interseismic velocity field. *Geochim. Geophys. Geosyst.* 2, doi:10.1029/2001GC000198.
- Bodine, J.H., 1981. Numerical Computation of Plate Flexure in Marine Geophysics. Technical Report NO 1, CU-1-80, Lamont-Doherty Geological Observatory, Columbia University.
- Brasse, H., Lezaeta, P., Rath, V., Schwalenberg, K., Soyer, W., Haak, V., 2002. The Bolivian Altiplano conductivity anomaly. *Journal of Geophysical Research* 107 (B5), doi:10.1029/2001JB000391.
- Burov, E., Diament, M., 1995. The effective elastic thickness (T_e) of continental lithosphere: what does it really mean? *Journal of Geophysical Research* 100 (B3), 3905–3927.
- Byerlee, J.D., 1978. Friction of rocks. *Pure and Applied Geophysics* 116, 615–626.
- Cahill, T., Isacks, B., 1992. Seismicity and shape of the subducted Nazca plate. *Journal of Geophysical Research* 97 (B12), 17503–17529.
- Carter, N., Tsenn, M., 1987. Flow properties of continental lithosphere. *Tectonophysics* 136, 27–63.
- Creager, K., Chiao, L., Winchester, J., Engdahl, R., 1995. Membrane strain rate in the subducting plate beneath South America. *Geophysical Research Letters* 22 (16), 2321–2324.
- Cristallini, E., Ramos, V., 2000. Thick-skinned and thin-skinned thrusting in the La Ramada fault and thrust belt: crustal evolution of the High Andes of San Juan, Argentina (32°S). *Tectonophysics* 317, 205–305.
- David, C., Martinod, J., Comte, D., Herail, G., Haessler, H., 2002. Intracontinental seismicity and Neogene deformation of the Andean forearc in the region of Arica (18.5°S–19.5°S). *V*

- International Symposium of Andean Geodynamics, Toulouse, France, pp. 171–174.
- de Silva, S., 1989. Altiplano–Puna volcanic complex of the Central Andes. *Geology* 17, 1102–1106.
- Fariás, M., Charrier, R., Comte, D., Martinod, J., Hérail, G., in press. Late Cenozoic uplift of the western flank of the Altiplano: evidence from the depositional, tectonic and geomorphologic evolution and shallow seismic activity. *Tectonics*.
- Froidevaux, C., Isacks, B., 1984. The mechanical state of the lithosphere in the Altiplano–Puna segment of the Andes. *Earth and Planetary Science Letters* 71, 305–314.
- García, M., Hérail, G., 2001. Comment on ‘Geochronology (Ar–Ar, K–Ar and He-exposure ages) of Cenozoic magmatic rocks from northern Chile (18–22°S): implications for magmatism and tectonic evolution of the central Andes’ of Wörner et al. (2000). *Revista Geológica Chilena* 28 (1), 127–130.
- García, M., Hérail, G., Charrier, R., Mascle, G., Fornari, M., Perez de Arce, C., 2002. Oligocene–Neogene tectonic evolution of northern Chile (18°–19°S). Fifth International Symposium of Andean Geodynamics, Toulouse, France, pp. 235–237.
- Gephard, J., 1994. Topography and subduction geometry of the Central Andes: clues to the mechanics of a non-collisional orogen. *Journal of Geophysical Research* 99, 12279–12288.
- Giambiagi, L., Ramos, V., 2002. Structural evolution of the Andes in a transitional zone between flat and normal subduction (33°30′–33°45′S), Argentina and Chile. *Journal of South American Earth Sciences* 15, 101–116.
- Giese, P., Scheuber, E., Schilling, F., Schmitz, M., Wigger, P., 1999. Crustal thickening process in the Central Andes and the different natures of the Moho-discontinuity. *Journal of South American Earth Sciences* 12, 201–220.
- Götze, H.-J., Kirchner, A., 1997. Interpretation of gravity and geoid in the Central Andes between 20° and 29°S. *Journal of South American Earth Sciences* 10 (2), 179–188.
- Götze, H.-J., Krause, S., 2002. The Central Andean gravity high, a relic of an old subduction complex? *Journal of South American Earth Sciences* 14, 799–811.
- Götze, H.-J., Lahmeyer, B., Schmidt, S., Strunk, S., 1994. The lithospheric structure of the Central Andes (20°–26°S) as inferred from interpretation of regional gravity. In: Reutter, K., Scheuber, E., Wigger, P. (Eds.), *Tectonics of the Southern Central Andes*. Springer-Verlag, Berlin, Germany.
- Gutscher, M.-A., 2002. Andean subduction styles and their effect on thermal structure and interplate coupling. *Journal of South American Earth Sciences* 15, 3–10.
- Gutscher, M.-A., Spakman, W., Bijwaard, H., Engdahl, R., 2000. Geodynamics of flat subduction: seismicity and tomographic constraints from the Andean margin. *Tectonics* 19 (5), 814–833.
- Hamza, V., Muñoz, M., 1996. Heat flow map of South America. *Geothermics* 25, 599–646.
- Handy, M., 1990. The solid-state flow of polymineralic rocks. *Journal of Geophysical Research* 95 (B6), 8647–8661.
- Hartley, A., Geoffrey, M., Chong, G., Turner, S., Kape, S., Jolley, E., 2000. Development of a continental forearc: a Cenozoic example from the Central Andes, northern Chile. *Geology* 28, 331–334.
- Henry, S.G., Pollack, H.N., 1988. Terrestrial heat flow above the Andean Subduction Zone in Bolivia and Peru. *Journal of Geophysical Research* 93 (B12), 15153–15162.
- Hérail, G., Oller, J., Baby, P., Bonhomme, M., Soler, P., 1996. Strike-slip faulting, thrusting and related basins in the Cenozoic evolution of the southern branch of the Bolivian Orocline. *Tectonophysics* 259, 201–212.
- Hindle, D., Kley, J., Klosko, E., Stein, S., Dixon, T., Norambuena, E., 2002. Consistency of geologic and geodetic displacements during Andean orogenesis. *Geophysical Research Letters* 29 (8), doi:10.1029/2001GL013757.
- Houseman, G., England, P., 1993. Crustal thickening versus lateral expulsion in the Indian–Asian continental collision. *Journal of Geophysical Research* 98 (B7), 12233–12249.
- Isacks, B., 1988. Uplift of the Central Andes plateau and bending of the Bolivian Orocline. *Journal of Geophysical Research* 93, 3211–3231.
- Jacay, J., Sempere, T., Husson, L., Pino, A., 2002. Structural characteristics of the Incapucio fault system, southern Peru. V International Symposium of Andean Geodynamics, Toulouse, France, pp. 319–321.
- Jackson, J., 2002. Strength of the continental lithosphere: time to abandon the jelly sandwich? *GSA Today*, 4–10.
- Jordan, T., Allmendinger, R., 1986. The Sierras Pampeanas of Argentina: a modern analogue of rocky mountain foreland deformation. *American Journal of Science* 286, 737–764.
- Jordan, T., Isacks, B., Allmendinger, R., Brewer, J., Ramos, V., 1983. Andean tectonics related to geometry of the subducted Nazca plate. *Geological Society of America Bulletin* 94, 341–361.
- Kay, S., Mpodozis, C., 2002. Magmatism as a probe to the neogene shallowing of the Nazca plate beneath the modern Chilean flat-slab. *Journal of South American Earth Sciences* 15, 39–57.
- Kay, S., Mpodozis, C., Coira, B., 1999. Neogene magmatism, tectonism and mineral deposits of the Central Andes (22°–33°S Latitude). In: Skinner, B. (Ed.), *Geology and Ore Deposits of the Central Andes*, Society of Economic Geology Special Publication, vol. 7, pp. 27–59.
- Kley, J., Monaldi, C., Salfity, J., 1999. Along-strike segmentation of the Andean foreland, causes and consequences. *Tectonophysics* 301, 75–94.
- Klotz, J., Khazaradze, G., Angermann, D., Reigber, R., Perdomo, R., Cifuentes, O., 2001. Earthquake cycle dominates contemporary crustal deformation in the Central and southern Andes. *Earth and Planetary Science Letters* 193, 437–446.
- Kösters, M., 1999. 3D-dichtemodellierung des Kontinentalrandes sowie quantitative Untersuchungen zur Rigidität der Zentralen Andean (20°–26°S). PhD thesis (unpublished), Freie Universität Berlin, 181 p.
- Kusznir, N., Karner, G., 1985. Dependence of the flexural rigidity of the continental lithosphere on rheology and temperature. *Nature* 316, 138–142.
- Lamb, S., 2000. Active deformation in the Bolivian Andes, South America. *Journal of Geophysical Research* 105 (B11), 2653–2667.
- Lamb, S., 2001. Vertical axis rotation in the Bolivian orocline, South America: 1. Paleomagnetic analysis of Cretaceous and

- Cenozoic rocks. *Journal of Geophysical Research* 106 (B11), 26605–26632.
- Lamb, S., Hoke, L., 1997. Origin of the high plateau in the Central Andes, Bolivia, South America. *Tectonics* 16, 623–649.
- Lucassen, F., Becchio, R., Harmon, R., Kasemann, S., Franz, G., Trumbull, R., Wilke, H., Romer, R., Dulska, P., 2001. Composition and density model of the continental crust at an active continental margin—the Central Andes between 21° and 27°S. *Tectonophysics* 341, 195–223.
- Marret, R., Strecker, M., 2000. Response of intracontinental deformation in the central Andes to late Cenozoic reorganization of South American Plate motions. *Tectonics* 19 (3), 452–467.
- McQuarrie, N., 2002. The kinematic history of the Central Andean fold-thrust belt, Bolivia: implications for building a high plateau. *GSA Bulletin* 114 (8), 950–963.
- Mpodozis, C., Kay, S., 1990. Provincias magmáticas ácidas y evolución tectónica de Gondwana: Andes chilenos (28°–31°S). *Revista Geológica de Chile* 17 (2), 153–180.
- Mpodozis, C., Ramos, V., 1989. The Andes of Chile and Argentina. In: Ericksen, G., Cañas-Pinochet, M., Reinemund, J. (Eds.), *Geology of the Andes and its Relation to Hydrocarbon and Mineral Resources*, Circum-Pacific Council for Energy and Mineral Resources Earth Sciences Series, vol. 11, pp. 59–90.
- Müller, R.D., Roest, W.R., Royer, J.-Y., Gahagan, L.M., Sclater, J.G., 1997. Digital isochrons of the world's ocean floor. *Journal of Geophysical Research* 102, 3211–3214.
- Muñoz, N., Charrier, R., 1996. Uplift of the western border of the Altiplano on a west-vergent thrust system, northern Chile. *Journal of South American Earth Sciences* 9, 171–181.
- Norabuena, E., Leffer-Griffin, L., Mao, A., Dixon, T., Stein, S., Sacks, S., Ocola, L., Ellis, M., 1998. Space geodetic observations of Nazca–South America convergence across the Central Andes. *Science* 279, 358–362.
- Pardo, M., Comte, D., Monfret, T., Boroscehk, R., Astroza, M., 2002a. The October 15, 1997 Punitaqui earthquake (Mw=7.1): a destructive event within the subducting Nazca plate in central Chile. *Tectonophysics* 345, 199–210.
- Pardo, M., Monfret, T., Vera, E., Eisenberg, A., Gaffet, S., Lorca, E., Perez, A., 2002b. Flat-slab subduction zone in Central Chile–Argentina: seismotectonic and body-wave tomography from local data. V International Symposium on Andean Geodynamics, Toulouse France, Extended Abstract. pp. 469–473.
- Pardo-Casas, F., Molnar, P., 1987. Relative motion of the Nazca (Farallon) and South American plates from Late Cretaceous time. *Tectonics* 6 (3), 233–248.
- Peacock, S., 1996. Thermal and petrologic structure of subduction zones (overview). In: Bebout, G., Scholl, D., Kirby, S., Platt, J. (Eds.), *Subduction, Top to Bottom*, Geophysical Monograph, vol. 96. American Geophysical Union.
- Pfiffner, O., Ramsay, J., 1982. Constraints on geological strain rates: arguments from finite strain states of naturally deformed rocks. *Journal of Geophysical Research* 87 (B1), 311–321.
- Porth, R., 2000. A strain-rate-dependent force model of lithospheric strength. *Geophysical Journal International* 141, 647–660.
- Ramos, V., Cristallini, E., Pérez, D., 2002. The Pampean flat-slab of the Central Andes. *Journal of South American Earth Sciences* 15, 59–78.
- Ranalli, G., 1987. Rheology of the earth, deformation and flow process in geophysics and geodynamics. Allen & Unwin.
- Ranalli, G., 1994. Nonlinear flexure and equivalent mechanical thickness of the lithosphere. *Tectonophysics* 240, 107–114.
- Roperch, P., Fornari, M., Herail, G., Parraguez, G., 2000. Tectonic rotations within the Bolivian Altiplano: implications for the geodynamic evolution of the central Andes during the late Tertiary. *Journal of Geophysical Research* 105, 795–820.
- Schurr, B., Asch, G., Rietbrock, A., Kind, R., Pardo, M., Heit, B., Monfret, T., 1999. Seismicity and average velocities beneath the Argentine Puna plateau. *Geophysical Research Letters* 26 (19), 3025–3028.
- Smith, W., Sandwell, D., 1997. Global seafloor topography from satellite altimetry and ship depth soundings. *Science* 277, 1957–1962.
- Somoza, R., 1998. Updated Nazca (Farallon)–South America relative motions during the last 40 My: implications for the mountain building in the central Andean region. *Journal of South American Earth Sciences* 11 (3), 211–215.
- Springer, M., 1999. Interpretation of heat-flow density in the Central Andes. *Tectonophysics* 306, 377–395.
- Springer, M., Förster, A., 1998. Heat-flow density across the central Andean subduction zone. *Tectonophysics* 291, 123–139.
- Stewart, J., Watts, A.B., 1997. Gravity anomalies and spatial variations of flexural rigidity at mountain ranges. *Journal of Geophysical Research* 102 (B3), 5327–5352.
- Swenson, J., Beck, S., Zandt, G., 2000. Crustal structure of the Altiplano from broadband regional waveform modeling: implications for the composition of thick continental crust. *Journal of Geophysical Research* 105 (B1), 607–621.
- Tapponnier, P., Peltzer, G., Armijo, R., 1986. On the mechanics of the collision between India and Asia. In: Coward, M.C., Ries, A.C. (Eds.), *Collision Tectonics*, Spec. Publ.-Geol. Soc. Lond., vol. 19, pp. 115–157.
- Tassara, A., 1997. Segmentación andina desde el análisis flexural de la anomalía de Bouguer. MsSci thesis, Universidad de Chile, Departamento de Geología, 140 p.
- Tassara, A., Yañez, G., 1996. Thermomechanic segmentation of the Andes (15°–50°S): a flexural analysis approach. III International Symposium on Andean Geodynamics, St. Malo, France, pp. 115–118.
- Tassara, A., Yañez, G., 2003. Relación entre el espesor elástico de la litósfera y la segmentación tectónica del margen andino (15–47°S). *Revista Geológica de Chile* 30 (2), 159–186.
- Tebbens, S., Cande, S., 1997. Southeast Pacific tectonic evolution from early oligocene to present. *Journal of Geophysical Research* 102 (B6), 12061–12084.
- Turcotte, D., Shubert, G., 1982. *Geodynamics, applications of continuum physics to geological problems*. John Wiley & Sons. 450 pp.
- USGS, EROS data centre. 1996. GTOPO30 (edition 1): Sioux Falls, South Dakota, U.S. Geological Survey. <http://www.edcdaac.usgs.gov/topo30/topo30.html>.

- Vanderhaeghe, O., Medvedev, S., Fullsack, P., Beaumont, C., Jamieson, R.A., 2003. Evolution of orogenic wedges and continental plateaux: insights from crustal thermal–mechanical models overlying subducting mantle lithosphere. *Geophysical Journal International* 153, 27–51.
- Vergés, J., Ramos, V.A., Bettini, F., Meigs, A., Cristallini, E., Cortés, J.M., Dunai, T., 2002. Geometría y edad del anticlinal fallado de Cerro Salinas. In: Cabaleri, N., Cingolani, C.A., Linares, E., López de Luchi, M.G., Ostera, H.A., Panarello, H.O. (Eds.), *Actas del XV Congreso Geológico Argentino CD-ROM*, Artículo No 358, 5 pp.
- Victor, P., Oncken, O., Glodny, J., 2004. Uplift of the western Altiplano plateau: Evidence from the Precordillera between 20° and 21°S (northern Chile). *Tectonics* 23 (TC4004), doi:10.1029/2003TC001519.
- Vietor, T., Oncken, O., 2002. Numerical modelling of Plateau kinematics in the Central Andes. V International Symposium on Andean Geodynamics, Toulouse, France, pp. 685–688.
- von Huene, R., Weinrebe, W., Heeren, F., 1999. Subduction erosion along the North Chile margin. *Geodynamics* 27, 345–358.
- Watts, A., 2001. *Isostasy and Flexure of the Lithosphere*. Cambridge University Press, 458 p.
- Wessel, P., Smith, W., 1998. New, improved version of generic mapping tools released. *EOS Transactions-American Geophysical Union* 79 (47), 579.
- Withman, D., Isacks, B., Kay, S., 1996. Lithospheric structure and along-strike segmentation of the Central Andean Plateau: seismic Q, magmatism, flexure, topography and tectonics. *Tectonophysics* 259, 29–40.
- Wörner, G., Seyfried, H., 2001. Reply to the Comment by M. García and G. Hérail on ‘Geochronology (Ar–Ar, K–Ar and He-exposure ages) of Cenozoic magmatic rocks from northern Chile (18–22°S): implications for magmatism and tectonic evolution of the central Andes’ by Wörner et al. (2000). *Revista Geológica de Chile* 28 (2), 131–137.
- Wörner, G., Hammerschmidt, K., Henjes-Kunst, F., Lezaun, J., Wilke, H., 2000. Geochronology (Ar–Ar, K–Ar and He-exposure ages) of Cenozoic magmatic rocks from northern Chile (18–22°S): implications for magmatism and tectonic evolution of the central Andes. *Revista Geológica de Chile* 27 (2), 205.
- Wörner, G., Uhlig, D., Kohler, I., Seyfried, H., 2002. Evolution of the West Andean Scarpment at 18°S (N. Chile) during the last 25 Ma: uplift, erosion and collapse through time. *Tectonophysics* 345, 183–198.
- Yáñez, G., Ranero, C., von Huene, R., Díaz, J., 2001. Magnetic anomaly interpretation across the southern Central Andes (32°–33.5°S): the role of the Juan Fernandez ridge in the late Tertiary evolution of the margin. *Journal of Geophysical Research* 106, 6325–6345.
- Yáñez, G., Cembrano, J., Pardo, M., Ranero, C., Selles, D., 2002. The Challenger–Juan Fernández–Maipo major tectonic transition of the Nazca–Andean subduction system at 33–34°S: geodynamic evidence and implications. *Journal of South American Earth Sciences* 15, 23–38.
- Yuan, X., Sobolev, S., Kind, R., Oncken, O., et al., 2000. Subduction and collision processes in the Central Andes constrained by converted seismic phases. *Nature* 408 (21/28), 958–961 (Diciembre).
- Yuan, X., Sobolev, S., Kind, R., 2002. Moho topography in the central Andes and its geodynamic implications. *Earth and Planetary Science Letters* 199, 389–402.
- Zandt, G., Velasco, L., Beck, S., 1994. Composition and thickness of the southern Altiplano crust, Bolivia. *Geology* 22, 1003–1006.